A Peptide Motif Consisting of Glycine, Alanine, and Valine Is Required for the Fibrillization and Cytotoxicity of Human α-Synuclein†

Hai-Ning Du,‡ Lin Tang,§ Xiao-Ying Luo,‡ Hong-Tao Li,‡ Jun Hu,§,|| Jia-Wei Zhou,‡ and Hong-Yu Hu*,‡

Key Laboratory of Proteomics, Institute of Biochemistry and Cell Biology, Shanghai Institutes for Biological Sciences, Chinese Academy of Sciences, Shanghai 200031, Shanghai Institute of Nuclear Research, Shanghai, and Bio-X Research Center, Shanghai Jiaotong University, Shanghai, PRC

Received January 9, 2003; Revised Manuscript Received May 28, 2003

ABSTRACT: Amyloid-like aggregation or fibrillization of α-synuclein (α-Syn) and the filamentous deposits in Lewy bodies are believed to be closely associated with several fatal neurodegenerative disorders, including Parkinson's disease and Alzheimer's disease. Here, we report the importance of a nine-residue peptide motif, ^{66}VGGAVVTGV^{74}, in the fibrillization and cytotoxicity of human α-Syn. Mutagenesis combined with thioflavin T fluorescence detection, atomic force microscopic imaging, and cytotoxicity assays reveal that deletion of this sequence completely eliminates α-Syn fibrillization and cell toxicity. However, deletion of the ^{71}VTGV^{74} sequence decreases the fibrillization rate while the cytotoxicity remains unchanged. Incorporation of charged residues within this region slows aggregation and even impedes filament formation. In addition, substitution of Gly68 with Ala or C-terminal truncations of α-Syn accelerate the fibrillization processes. Circular dichroism studies suggest that *β*-sheet formation is often concomitant with filament formation. Thus, this segment, namely, the GAV motif, is responsible for aggregation or fibrillization of α-Syn and perhaps other amyloidogenic proteins. The oligomers formed during fibrillogenesis might be associated with the cytotoxicities of various α-Syn species. This finding may provide further insight into the understanding of the molecular mechanism underlying the fibrillogenesis implicated in neurodegeneration as well as aid in drug design and development of transgenic models.

Protein amyloidogenesis or fibrillogenesis is generally considered a major cause of some fatal neurodegenerative disorders (*1*, *2*), such as Alzheimer's disease (AD),[1] Parkinson's disease (PD), and prion diseases. Among the disease-associated amyloidogenic proteins, α-synuclein (α-Syn) is closely associated with PD, the Lewy body (LB) variant of AD, dementia with LB, and multiple-system atrophy (*3*). The pathological hallmarks of these disorders are the presence of Lewy bodies and Lewy neurities (*4*). These observations have attracted extensive attention in investigating the potential relationship between α-Syn fibrillization and human neurodegenerative diseases.

Recent studies have shown that α-Syn (*5*, *6*), as well as amyloid *β*-protein (A*β*) (*7*) and prion protein (PrP) (*8*), is prone to aggregation or even fibrillization *in vitro* (*9*). Some disease-associated mutations have proven to accelerate the aggregation process (*10*, *11*) or oligomerization but not fibrillization (*12*). A growing body of evidence supports the idea that A*β* plays a primary causal role in the progression of AD (refs *13* and *14* and references therein). Aggregation of PrP is also associated with the pathogenesis of human and other mammalian prion diseases (*15*). These findings motivated us to further investigate the relationship between amino acid sequences and fibrillogenesis of these neurodegeneration-related proteins, but to date, there are still pieces of the puzzle unsolved (*16*). The GAXX motif was first identified as a core region that is crucial to aggregation of some amyloidogenic proteins (*17*, *18*). In addition, a recent study suggested that a stretch of residues 71−82 of α-Syn is related to aggregation (*19*).

It is well-known that the nonamyloid component (NAC) sequence (residues 61−95) of α-Syn is the core region responsible for fibrillization (*17*). To further investigate the relationship between the amino acid sequence in the NAC region and the biochemical properties of aggregation or fibrillization, we focused on a novel sequence in human α-Syn (residues 66−74). We have named the nine-residue peptide segment the GAV motif, as it mainly contains three kinds of amino acid residues, glycine (G), alanine (A), and valine (V). Secondary structural prediction suggests that the GAV segment has the propensity to form *β*-strand structure (*6*). Since α-Syn is natively unfolded (*20*), investigators have

† Supported by grants from the National Natural Science Foundation of China (NSFC39990600 and NSFC39930060) and the Chinese Academy of Sciences (STZ97-2-02 and STZ00-07).

* To whom correspondence should be addressed. Telephone: 86-021-54921121. Fax: 86-021-54921011. E-mail: hyhu@sibs.ac.cn or hyhu@sunm.shcnc.ac.cn.

‡ Shanghai Institutes for Biological Sciences.

§ Shanghai Institute of Nuclear Research.

|| Shanghai Jiaotong University.

[1] Abbreviations: A*β*, amyloid *β*-protein; AD, Alzheimer's disease; AFM, atomic force microscopy; CD, circular dichroism; DLB, dementia with LB; DMEM, Dulbecco's modified Eagle's medium; DMF, *N*,*N*-dimethylformamide; LB, Lewy body; MTT, 3-(4,5-dimethylthiazol-2-yl)-2,5-diphenyltetrazolium bromide; NAC, nonamyloid component; PBS, phosphate-buffered saline; PD, Parkinson's disease; PrP, prion protein; α-Syn, human α-synuclein; *γ*-Syn, human *γ*-synuclein; ThT, thioflavin T; WT, wild type.

10.1021/bi034028+ CCC: $25.00
Published on Web 07/01/2003

speculated that the GAV segment is involved in a structural transformation from random coil to β-sheet that is likely accompanied by amyloid fibrillization. By means of mutagenesis in combination with thioflavin T (ThT) fluorescence detection, atomic force microscopy (AFM) imaging, circular dichroism (CD) spectroscopy, and cytotoxicity assays, we demonstrate that the GAV peptide motif is essential for α-Syn fibrillization and cytotoxicity. Possible applications to studies of Aβ, PrP, and other amyloidogenic proteins are also discussed.

MATERIALS AND METHODS

Cloning, Bacterial Expression, and Purification of Synucleins. All recombinant synuclein genes were subcloned into the pET3a vector, and the respective proteins were expressed in *Escherichia coli* BL21(DE3). All mutants, including C-terminally truncated forms and forms with residues 66−74 and 71−74 deleted, were generated by site-directed mutagenesis using polymerase chain reaction. For the sake of detection in purification and quantification, a Phe4Trp mutation was introduced into the truncated proteins. The gene sequences encoding the target proteins were confirmed by DNA sequencing. Recombinant human α-Syn and γ-synuclein (γ-Syn) were prepared as described elsewhere (*20*, *21*). The truncated proteins, including α-Syn$_{1-60}$, α-Syn$_{1-70}$, α-Syn$_{1-74}$, and α-Syn$_{1-100}$, were purified through a CM-Sephadex C25 cation-exchange column. The fractions containing α-Syn were further purified with a FPLC Superose-12 column (Amersham) with PBS buffer [100 mM phosphate and 100 mM NaCl (pH 7.0)]. The homogeneity of the α-Syn proteins was identified by SDS−PAGE and mass spectrometry, and the concentrations of the proteins were determined by measuring the absorbance at 280 nm using extinction coefficients calculated according to the amino acid sequences.

Time Course of the Aggregation Processes. All the protein samples were concentrated to ca. 3 mg/mL by using Centricon YM-3 spin filters (Millipore) in PBS buffer with 0.05% sodium azide and then sterilely filtered through 0.22 μm filters to remove any granular matter. The filtrates were incubated in 1.5 mL sterile tubes with continuous shaking at 37 °C. With the incubation progressing, aliquots of each protein were taken and stored at −20 °C at various time points. The time course of the aggregation process was monitored by a ThT (Aldrich) fluorescence assay (*22*). The enhancement of ThT fluorescence was used to semiquantitatively estimate the relative rate of filament formation. Fluorescence measurements were performed on a Hitachi F-4010 fluorophotometer. A ThT stock solution (100 μM) was prepared and filtered through a 0.22 μm filter. Each 20 μL of the incubated samples was added to 980 μL of 5 μM ThT in 50 mM glycine-NaOH buffer (pH 9.0). The emission intensities at 482 nm were recorded immediately after addition of the aliquots to the ThT solution with excitation at 446 nm. Sedimentation analysis of various α-Syn species was carried out with an ultracentrifuge. Aliquots of the incubated samples were centrifuged at 100000*g* for 20 min, and then SDS−PAGE of the supernatants (S) and pellets (P) was performed on 15% polyacrylamide gel and stained with Coomassie Blue.

Circular Dichroism Measurements. Far-UV CD measurements were performed on a JASCO-715 spectropolarimeter as described previously (*21*). The protein samples (200 μM) with a 6 day incubation were diluted 1:20 in doubly distilled water and transferred to a 0.1 cm quartz cuvette. The nonincubation sample was used as a comparison. For each spectrum, an average of two scans was obtained, and the data were presented as the mean residue molar ellipticity (deg cm^2/dmol).

Atomic Force Microscopy. All synuclein proteins were diluted to 10 μM with PBS buffer. Each sample was prepared by depositing 5 μL of the solution on freshly cleaved mica (Alfa Aesar). After adsorption for 5 min, the mica surface was gently washed with deionized water, to remove redundant buffer and the protein that was not firmly attached to the surface. Excess water was removed with condensed air. Images were obtained at a commercial AFM facility (nanoscope III, Digital Instruments, Santa Barbara, CA) equipped with a 130 μm × 130 μm scanner (J-scanner) by tapping mode imaging. The cantilevers with a nominal force constant κ of 20−100 N/m were purchased from Digital Instruments. Each sample was observed in at least five regions to avoid experimental error. Normally, scanning parameters varied with individual tip and sample. Typical parameters were used in the experiments. The free oscillation amplitude was 20−40 mV, the set point 0.4−0.6 V, the drive (tapping) frequency 280−340 kHz, and the scan rate 1.1−2.5 Hz.

Cytotoxicity Assay. The cytotoxicities of the protein aggregates were determined as described previously (*23*). Briefly, PC12 cells (rat pheochromocytoma, American Type Culture Collection) were cultured in DMEM (Gibco BRL) supplemented with 6.0% horse serum and 10.0% fetal bovine serum in a 5.0% CO_2 humidified atmosphere at 37 °C. Penicillin (100 units/mL) and streptomycin (100 μg/mL) were included. PC12 cells were plated on the 48-well plates in 200 μL of fresh medium at a density of 10 000 cells per well. After 24 h, the medium was exchanged with 200 μL of DMEM without phenol red, supplemented with 6.0% horse serum and 10.0% fetal bovine serum. For assaying the cytotoxicities of various protein aggregates, each aliquot of the aggregated protein in PBS was added to the cell medium with a final concentration of 10 μM. After incubation for 24 h, an MTT solution was added to the cell culture to a final concentration of 0.5 mg/mL. After incubation for an additional 3 h, 1 volume of cell lysis buffer [20.0% SDS and 50.0% DMF (pH 4.7)] was added to each well, and the cultures were incubated overnight at 37 °C in a humidified incubator. Absorbance values at 570 nm were recorded (DU-7500 spectrophotometer, Beckman) for the MTT reduction of each cell culture.

RESULTS

NAC(61−95) Is the Core Region of α*-Syn Fibrillization.* As reported in the previous studies (*17*, *18*), α-Syn readily aggregates into fibrils as detected by a variety of biophysical methods. Figure 1A displays time courses of aggregation processes of wild-type (WT) α-Syn, two C-terminally truncated proteins (α-Syn$_{1-100}$ and α-Syn$_{1-60}$), and γ-Syn by a ThT fluorescence assay (*22*). Aggregation of α-Syn normally shows an S-form curve with a lag phase of 18−24 h and a completion time of 4−6 days. Truncation of the acidic C-terminus (α-Syn$_{1-100}$) may accelerate the aggregation without the presence of the lag phase. However, deletion

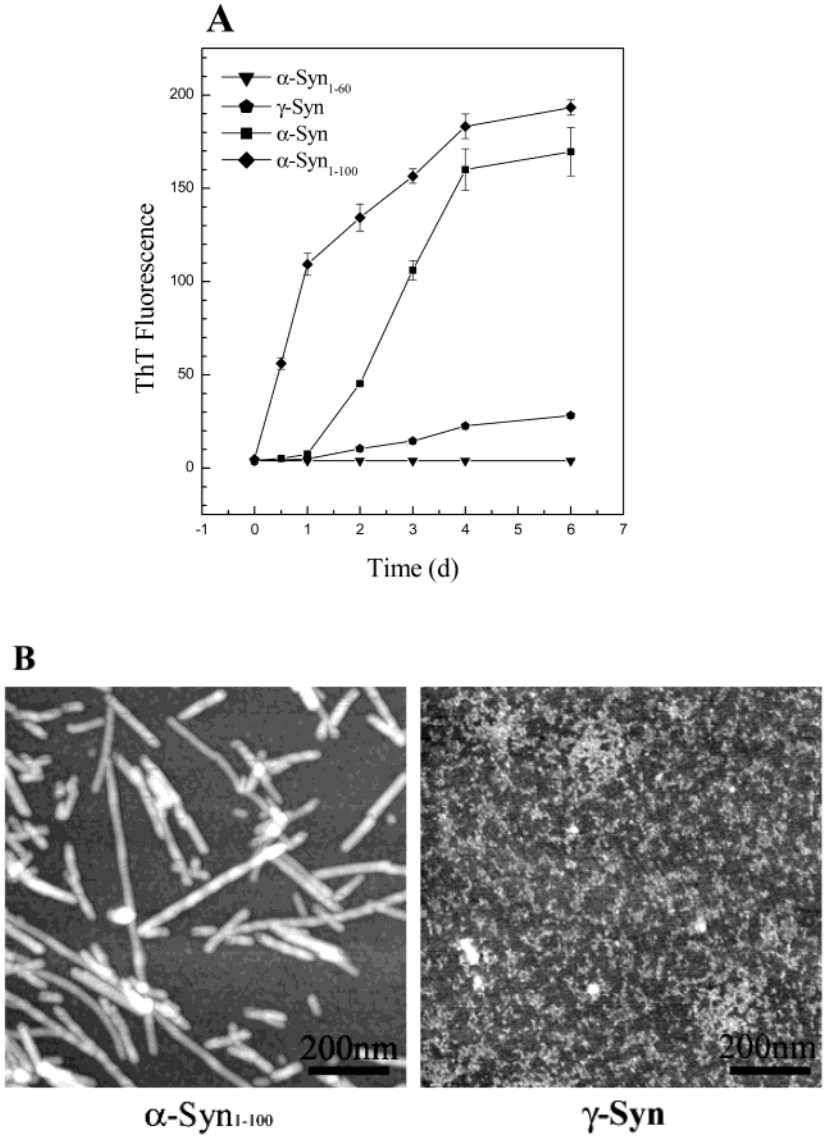

FIGURE 1: Central sequence of α-Syn (NAC) which is the core region of filament formation. (A) Time course of aggregation of intact α-Syn (■), α-Syn$_{1-60}$ (▼), and α-Syn$_{1-100}$ (◆) as determined by a ThT fluorescence assay. Data for γ-Syn (⬟) are shown for comparison. Data are the average of triplicate incubations (mean ± standard error, next as same). (B) Atomic force microscopic images of α-Syn$_{1-100}$ and γ-Syn. The samples were incubated for 6 days. α-Syn$_{1-100}$ gives a filamentous image similar to that of WT α-Syn, but γ-Syn can form only small-size particles. All graphs are topographical height images 1 μm^2 in area. The increasing brightness represents the increasing height of areas. The scale bar represents 200 nm (next as same).

of the NAC sequence (α-Syn$_{1-60}$) results in elimination of the aggregation ability. Although γ-Syn still has the ability to aggregate, the aggregation rate is rather low and the filamentous amount is very small as measured by ThT fluorescence. α-Syn$_{1-100}$, like WT α-Syn (see Figure 3A), can form highly ordered fibrils after incubation for several days (Figure 1B). γ-Syn, however, cannot generate filaments but forms amorphous aggregates with some small particles. The experimental results provide convincing evidence supporting the previous observations that NAC(61−95) is the core region of α-Syn fibrillization.

Effects of Incorporating Charged Residues into the GAV Motif Region on α-Syn Fibrillization. Previous studies *in vitro* indicated that aggregation of α-Syn could form fibrils with a lag phase roughly 3 times shorter than that of γ-Syn with vigorous shaking during incubation (*6*). Our current results reconfirm that γ-Syn does not spontaneously form fibrils (Figure 1). Comparing the amino acid sequences of α- and γ-Syn within the GAV motif region indicates that Gly68 in α-Syn is substituted with a negatively charged Glu residue in γ-Syn. We speculated that introducing charged residues into the region could reduce fibril formation. To test this hypothesis, a series of point mutants of α-Syn, i.e., G68E, G68R, V66R, V70R/V71R, and V74R, were generated by site-directed mutagenesis.

As expected, all the charged mutants show no obvious fluorescence enhancement even after incubation for 15 days as compared with WT α-Syn (Figure 2A,B). AFM imaging demonstrates that, after incubation for 6 days, human α-Syn forms abundant filaments with ∼10−20 nm in diameter and micrometer scale in length (Figure 3A), but no mature fibrils can be visualized in any of the charged mutants even after incubation for 15 days (Figure 3B). Instead, small short filaments of different sizes (10−20 nm in height and 50−160 nm in length) and amounts were occasionally found in V66R and G68R mutants (Figure 3C). Another group,

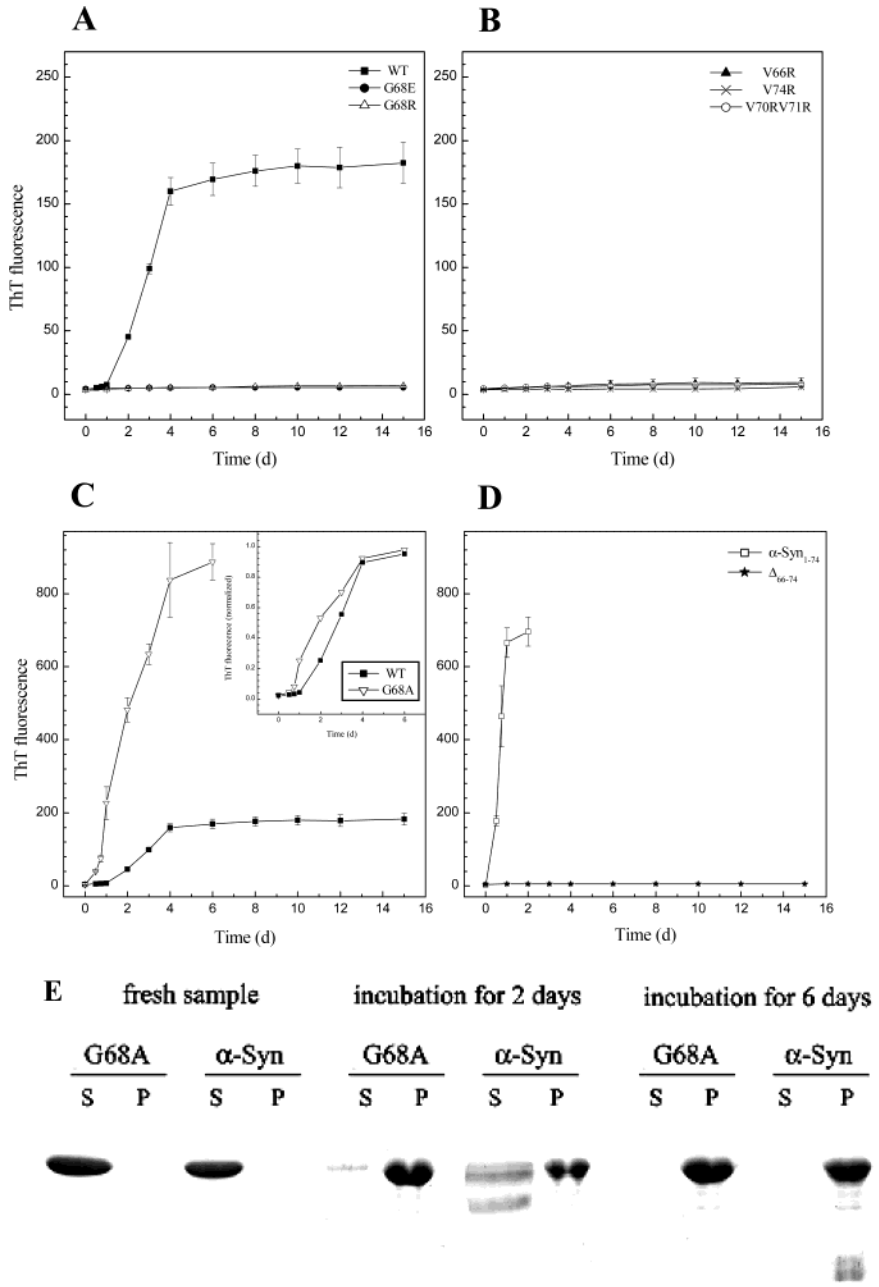

FIGURE 2: Time course of aggregation processes of α-Syn and its mutants as determined by the thioflavin T fluorescence assay and centrifugation sedimentation analysis: (A) WT α-Syn (■), G68E (●), and G68R (△); (B) V66R (▲), V74R (×), and V70R/V71R (○); (C) G68A (▽) and WT (■) (the inset shows the normalized ThT fluorescence comparing the aggregation rate of those two proteins); and (D) α-Syn$_{1-74}$ (□) and Δ_{66-74} (★). (E) SDS−PAGE graphs of G68A and WT α-Syn with different incubation times.

including G68E, V70R/V71R, and V74R, form small oligomers with a mean height of ~8 nm. In addition, CD spectra show that the five mutants have not experienced any conformational changes, retaining unfolded structures in the incubated samples similar to that of the fresh solution. Only WT α-Syn transforms into a *β*-sheet structure from the natively unfolded structure (Figure 4A−D). Taken together, these data demonstrate that introduction of charged residues in the GAV motif region indeed has a great impact on the rate and morphology of α-Syn fibrillization.

A Gly-to-Ala Mutation within the GAV Motif Significantly Accelerates α-Syn Fibrillization. Evidence described above supports the concept that substituting charged residues in the GAV region significantly perturbs fibrillogenesis of human α-Syn. To further investigate the nature of residues in α-Syn fibrillization, we reconstructed a G68A mutant. Interestingly, this mutation dramatically accelerates aggregation, when compared with WT α-Syn, with only a very short lag period during incubation as assayed by ThT fluorescence (Figure 2C). The inset is the time course of normalized fluorescence, showing the faster aggregation of the G68A mutant. The increase in ThT fluorescence intensity at 482 nm suggests that more ThT dyes are bound to the aggregates. A possible explanation is that incorporation of the Ala residue may increase the hydrophobicity of this region, and consequently improve the ThT binding ability. The sedimentation analysis combined with electrophoresis shows that G68A aggregates almost completely in a 2 day incubation, while WT α-Syn retains a substantial amount of supernatant (Figure 2E). AFM of the G68A sample after incubation for 2 days

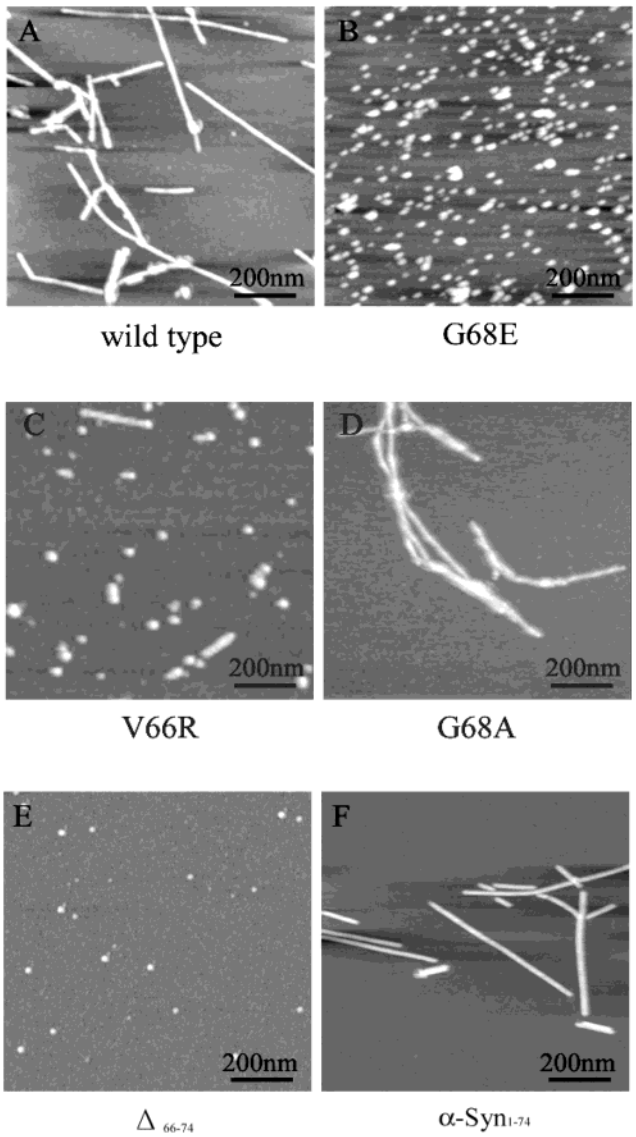

FIGURE 3: Atomic force microscopic images of fibrillization of α-Syn and its variants. The samples for AFM imaging were processed by continuous incubation for a different number of days (40 nm total *z*-range images for mature fibrils and 20 nm total *z*-range images for oligomers): (A) WT α-Syn for 6 days, (B) G68E for 15 days, (C) V66R for 15 days, (D) G68A for 2 days, (E) Δ_{66-74} for 15 days, and (F) α-Syn_{1-74} for 2 days (scale bar, 200 nm).

presents the morphology of filaments (Figure 3D) resembling that observed in the WT protein. As expected, CD studies also reveal that G68A undergoes a structural transformation from random coil to β-sheet, like WT α-Syn (Figure 4E,F). It appears that the third position of the GAV motif occupied by Ala rather than Gly is beneficial to α-Syn fibrillization.

GAV Sequence Deletion Eliminating α-Syn Fibrillization. To ascertain the significance of the GAV motif in driving filament formation, we generated two deletion variants of α-Syn, Δ_{66-74} (residues 66−74 deleted) and α-Syn_{1-74} (deletion of C-terminal residues 75−140). On incubation, Δ_{66-74} does not aggregate into filaments under the same condition with shaking at 37 °C, as monitored by a ThT fluorescence assay (Figure 2D). Consequently, AFM failed to reveal the presence of any filaments or oligomers in the sample after incubation for 15 days (Figure 3E), and even after prolonged incubation for more than 6 weeks (data not shown). On the contrary, α-Syn_{1-74} significantly accelerates fibril formation, resulting in the absence of the lag time (Figure 2D). The protein can cause a significant increase in ThT fluorescence intensity even within an incubation period of 12 h. Long regular filaments can be seen in a 2 day sample of α-Syn_{1-74} by AFM imaging (Figure 3F). All the deletion variants, as well as WT α-Syn, possess a predominantly random coil conformation in solution (Figure 4E). The CD spectra show that the GAV sequence deletion (Δ_{66-74}) results in the absence of β-sheet formation, whereas α-Syn_{1-74} gives a strong indication of β-sheet structure formation after incubation of the sample (Figure 4F). In comparison, the NAC sequence-truncated α-Syn_{1-60} is incapable of fibrillization (see Figure 1A). The results from mutagenesis and morphological visualization clearly indicate that the GAV motif is the critical core for α-Syn fibrillization.

The ^{71}VTGV^{74} Sequence Is Important but Not Sufficient for α-Syn Fibrillization. A previous report has suggested that the hydrophobic stretch of residues 71−82 is associated with aggregation (*19*). Actually, the GAV motif and the hydrophobic stretch share an overlapping sequence of ^{71}VTGV^{74}. To further ascertain the function of the GAV motif in α-Syn aggregation, we generated two other mutants: α-Syn_{1-70} and Δ_{71-74}. α-Syn_{1-70} aggregates at a rate that is slower than that of WT α-Syn (Figure 5A) and forms irregular fibrils with morphology different from those of WT even after prolonging the incubation time (Figure 5B). In addition, Δ_{71-74} can only form oligomers or a few short fibrils. There is also a conformational change that can be detected in α-Syn_{1-70} between the fresh and aged proteins, but not in Δ_{71-74} (Figure 5C,D). As compared with α-Syn_{1-74} which aggregates into regular fibrils with the fastest rate and the greatest abundance (Figure 3F), it is conclusive that the ^{71}VTGV^{74} sequence may play an important role in α-Syn fibrillization, but the entire GAV motif of nine residues seems to be required for formation of mature regular fibrils.

α-Syn Fibrillization Is Associated with Its Cytotoxicity. To confirm the function of the GAV motif in the aggregation of α-Syn, we examined the toxic effect of various α-Syn mutants on PC12 cells by using the MTT assay. Figure 6 shows the percentage of MTT reduction in PC12 cell cultures versus the incubation time of the mutant proteins. After treatment with α-Syn, G68R, or Δ_{71-74} preincubated for 2 days, the percentage of surviving cells is only ~60% of the untreated control. This suggests that WT α-Syn, G68R, and Δ_{71-74} have significant cytotoxicities on PC12 cells. Surprisingly, the Δ_{66-74} mutant has a weaker effect on the cell viability with almost 100% MTT reduction, even when the protein has been incubated for 6 days *in vitro*. This is in accordance with the above observation that Δ_{66-74} fails to form fibrils or even oligomers, while three other proteins (WT α-Syn, G68R, and Δ_{71-74}) can form aggregates despite having different aggregation rates and morphologies. We also examined the cytotoxicities of other charged mutants on PC12 cells and observed the equivalent toxic effect (data not shown). These results from the MTT assay imply that the cytotoxicities of the α-Syn mutants that have been examined might be associated with the oligomerization abilities, and the GAV sequence may play important roles in aggregation and cytotoxicity of α-Syn.

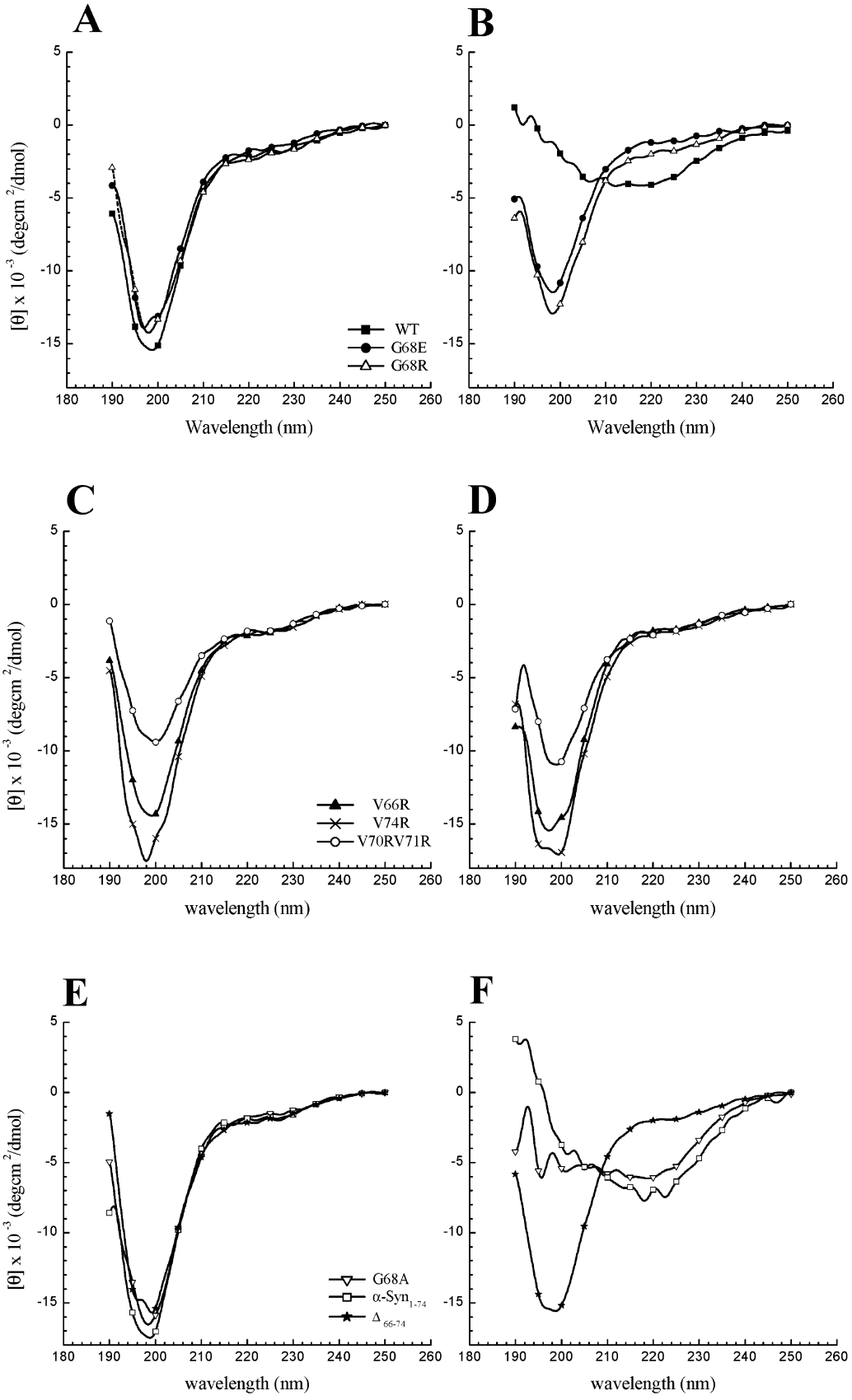

FIGURE 4: Circular dichroic spectra of α-Syn and its mutants showing the secondary structural changes form the soluble forms during the aggregation processes. The CD measurements were performed on the samples before (A, C, and E) and after (B, D, and F) incubation for 6 days (except for α-Syn$_{1-74}$, which was incubated for only 2 days) at 37 °C with continuous shaking as described in Materials and Methods: (A and B) WT α-Syn (■), G68E (●), and G68R (△); (C and D) V66R (▲), V74R (×), and V70R/V71R (○); and (E and F) G68A (▽), α-Syn$_{1-74}$ (□), and Δ_{66-74} (★).

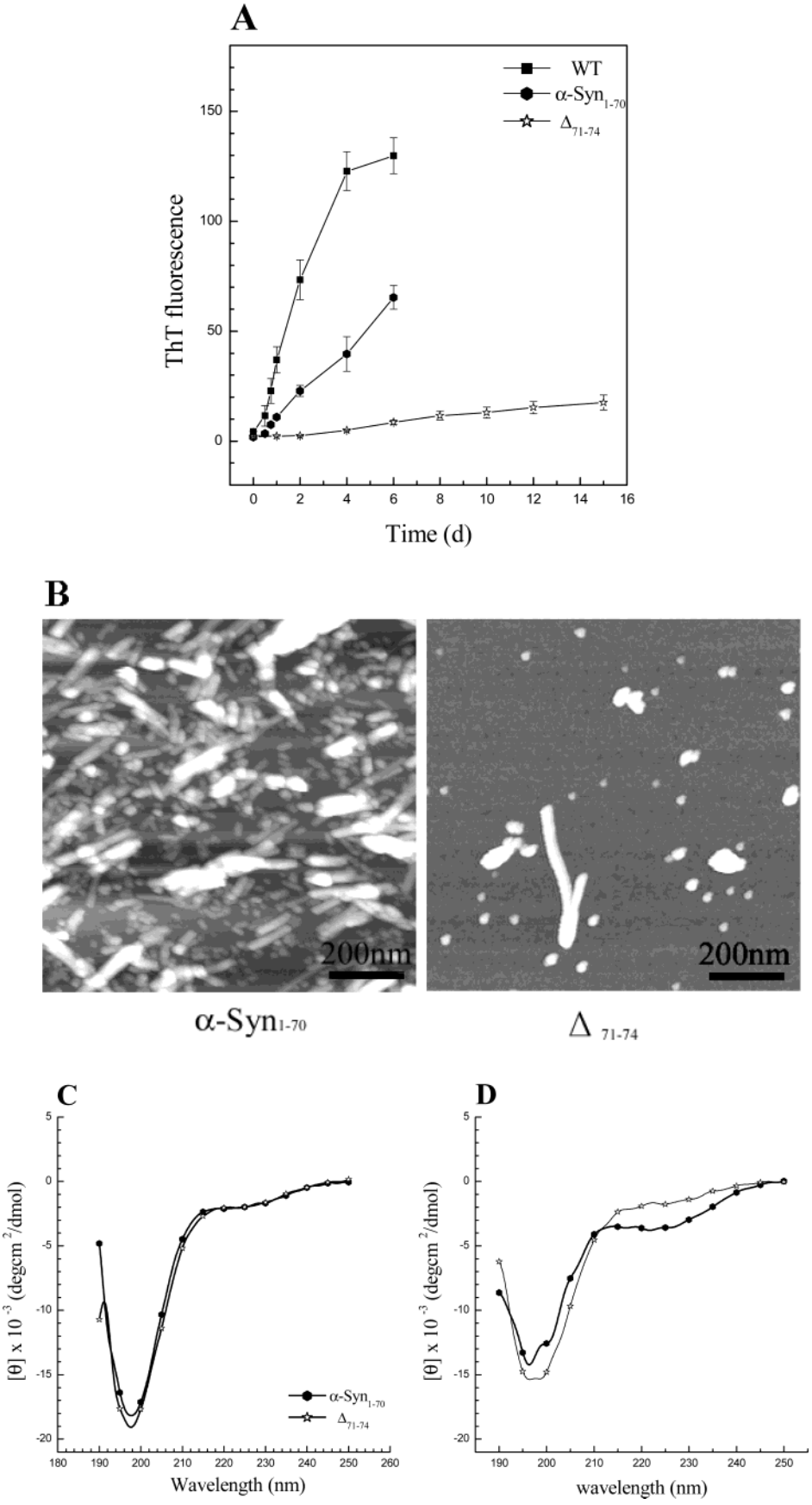

FIGURE 5: ^{71}VTGV^{74} sequence which is important but not sufficient for human α-Syn fibrillization. (A) Time course of aggregation of α-Syn (■), α-Syn$_{1-70}$ (⬢), and Δ_{71-74} (☆) as determined by the thioflavin T fluorescence assay. (B) AFM images of α-Syn$_{1-70}$ and Δ_{71-74} after incubation for 6 days (scale bar, 200 nm). (C and D) CD spectra of α-Syn$_{1-70}$ (⬢) and Δ_{71-74} (☆) recorded before (C) and after (D) incubation for 6 days.

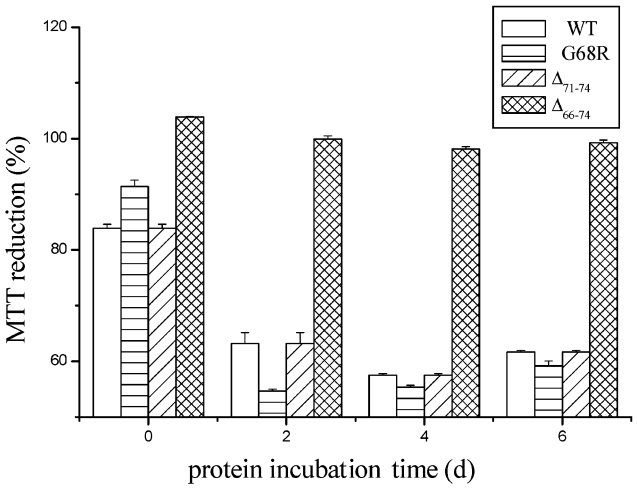

FIGURE 6: Cytotoxicities of α-Syn and its mutants. The aggregates were made by incubating the proteins in PBS buffer for the indicated number of days and added to the cell culture at a final concentration of 10 μM. The percentage of MTT reduction represents the cell viability after treatments of incubated protein aggregates ($p < 0.001$, $n = 3$). The MTT reduction ability of the cell culture without addition of protein was regarded as a control.

DISCUSSION

The amino acid sequence of α-Syn has three distinct regions. It seems that the N-terminal amphipathic repeats and the C-terminal acidic part are irrelevant to fibrillization (*24*). The central hydrophobic segment might be involved in initiating or seeding α-Syn fibrillization. In addition to our experimental results of α-Syn mutagenesis, other evidence also supports the viewpoint that the GAV-related sequence is essential for fibrillization and cytotoxicity (*25*). Some literature has reported that the C-terminally truncated but NAC-containing fragments of human α-Syn, such as α-Syn$_{1-120}$, α-Syn$_{1-87}$ (*26*), and α-Syn$_{1-100}$ (*27*), assemble with faster rates than the native intact α-Syn. It is likely that the GAV-containing fragment α-Syn$_{1-74}$ gives the highest self-assembly rate among these C-terminally truncated fragments; on the other hand, the GAV-breaking α-Syn$_{1-70}$ gives a much slower aggregation rate (but comparable with that of intact α-Syn) and GAV-lacking α-Syn$_{1-60}$ loses the self-assembly feature. It was reported that a deletion of residues 71−82 impeded polymerization of human α-Syn (*19*). Actually, this sequence partially overlaps the GAV motif. These four residues (71−74, VTGV) may play a role in the fibrillization since deletion of these four residues decelerates the aggregation rate but retains the self-assembly ability. These observations strongly demonstrate that the GAV motif is the critical core of human α-Syn fibrillization. Since α-Syn, Aβ, and PrP share a homologous hydrophobic region (*17*, *18*) [the central segment of α-Syn (residues 66−74), the C-terminus of the Aβ peptide (residues 36−44), and the conversion region of PrP (residues 117−125)], it is quite likely that the homologous sequence plays an important role in fibrillization of Aβ and PrP, although more work needs to be done on these proteins.

The GAV motif comprises nine amino acid residues. Gly is the most flexible residue; it may keep the sequence in a disordered structure in aqueous solution. Ala is a strong secondary structure former, and the hydrophobic Val has a propensity to form β-sheets. This unique sequence may be necessary for structural transformation from a random coil in aqueous solution into an aggregated β-sheet structure. Interestingly, an N-terminal polyalanine tract expansion of poly(A) binding protein 2 (PABP2) causes intranuclear inclusions which are pathogens in oculopharyngeal muscular dystrophy (OPMD) disease (*28*). Another example is the pulmonary surfactant protein-c (SP-C), which contains a polyvaline region in the central part and is associated with proteinosis, a respiratory disease (*29*). Similar sequences were also found in spider silks with GA/A (Ala-rich) and GGX/GPG (Gly-rich) repeats in the amino acid sequence (*30*), which can transform into dragline silk fibers from the soluble protein (*31*). Although we have no idea yet about whether all the proteins rich in Gly, Ala, and Val residues are susceptible to amyloid formation, it is likely not a coincidence that the GAV homologue appears in some potential amyloidogenic proteins responsible for neurodegeneration. To a lesser extent, amyloid-like aggregation of proteins is sequence specific (*32*). Aβ_{42}, by extending the Ile-Ala sequence of Aβ_{40} in the C-terminus, aggregates into fibrils with a much faster rate, and neurons with Aβ_{42} accumulation are extremely risky on AD (*33*). As for human PrP, it was proposed that the PrP region of residues 106−126 is crucial for prion conversion and neurotoxicity (*34*). Moreover, the chemically synthesized peptides corresponding to the GAV sequence in PrP (*35*) and Aβ (*36*) are highly amyloidogenic. Our recent experiments also indicate that the GAV homologous peptides are prone to secondary structural transformation and aggregation (unpublished data). However, incorporation of charged residue into the GAV region significantly reduces or eliminates α-Syn fibrillization. This allows us to consider the nature of the amino acid sequence in this local region when elucidating the mechanism underlying the neurodegeneration.

The common structural feature of the α-Syn variants and some amyloidogenic proteins (*20*, *37*) is that they all exhibit natively unfolded structures in the GAV homologue regions. Other amyloidogenic proteins such as yeast prion Sup35 (*38*) and Ure2P (*39*) also tend to form random coil structure in prion domains. The natively unstructured region (residues 117−125) in the N-terminus of PrP may act as a pivotal segment that would promote structural transition (*40*). Thus, the local disordered GAV segment may provide an opportunity for structural transformation and abnormal fibrillogenesis as β-sheet formation from random coil is usually concomitant with the fibrillogenic processes (*36*). These findings imply that a segment of high structural propensity but with a non-β-sheet structure in the native state tends to structural transformation, which readily aggregates into fibrils in concomitance with β-sheet structure formation. This is also corroborated by the CD studies demonstrating that α-Syn undergoes a transition from a disordered structure in solution to a fibril-like morphology with typical β-sheet structure in the solid state (*21*).

It was postulated that the early-stage aggregates are highly toxic to cellular function, and formation of inclusion bodies (such as LBs) prevents neurons from experiencing the toxicity of the oligomers (*41*−*43*). Our study also shows that formation of oligomeric aggregates can cause cell toxicity, but nonaggregation (Δ_{66-74}) may have a weaker effect on cell viability. This implies that the cytotoxicity of α-Syn corresponds to the degree of possible aggregation or perhaps

oligomerization, and these behaviors are likely associated with the GAV motif or other related regions (*18*, *25*). Some mutations can slow filament formation and even hamper the aggregation process so that α-Syn stays in the oligomeric form rather than proceeding to the fibril form. The oligomeric form of α-Syn might be extremely toxic, and therefore, storage of the aggregates may mitigate cell impairment. Once oligomeric proteins have accumulated in a cell, two possible processes may occur within the cell. One is to initiate the apoptosis pathway (*44*) and another to deposit the toxic oligomers in inclusion bodies.

This study provides evidence that a short nine-residue peptide segment within the NAC region indeed plays a central role in α-Syn fibrillization and cytotoxicity. This may open up the way to elucidating the mechanism underlying the fibrillization and cytotoxicity of α-Syn as well as other amyloidogenic proteins, and to explore effective therapeutic strategies for treatments. The novel sequence may be exploited as a potential target for the design of inhibitors that retard amyloidogenesis of GAV-motif related proteins and most likely mitigate progression of neurodegenerative diseases. A plausible application of the mutations is to transplant an altered α-Syn gene that expresses a nonamyloidogenesis protein into research animals by transgenic techniques. The putative transgenic animals with a specially modified gene might be developed as a PD or AD model for clinical research.

ACKNOWLEDGMENT

We thank Prof. G. J. Xu and M. Q. Li for encouragement and help in the research field and Miss Leila Mosavi for critical reading of the manuscript.

REFERENCES

1. Rochet, J. C., and Lansbury, P. T., Jr. (2000) *Curr. Opin. Struct. Biol*. *10*, 60−68.
2. Koo, E. H., Lansbury, P. T., Jr., and Kelly, J. W. (1999) *Proc. Natl. Acad. Sci. U.S.A. 96*, 9989−9990.
3. Dickson, D. W. (2001) *Curr. Opin. Neurol. 14*, 423−432.
4. Spillantini, M. G., Schmidt, M. L., Lee, V. M. Y., Trojanowski, J. Q., Jakes, R., and Goedert, M. (1997) *Nature 388*, 839−840.
5. Conway, K. A., Harper, J. D., and Lansbury, P. T., Jr. (2000) *Biochemistry 39*, 2552−2563.
6. Biere, A. L., Wood, S. J., Wypych, J., Steavenson, S., Jiang, Y., Narhi, L., Anafi, D., Jacobsen, F. W., Jarosinski, M. A., Wu, G. M., Louis, J. C., Martin, F., Narhi, L. O., and Citron, M. (2000) *J. Biol. Chem. 275*, 34574−34579.
7. Walsh, D. M., Hartley, D. M., Kusumoto, Y., Fezoui, Y., Condron, M. M., Lomakin, A., Benedek, G. B., Selkoe, D. J., and Teplow, D. B. (1999) *J. Biol. Chem. 274*, 25945−25952.
8. Harrison, P. M., Bamborough, P., Daggett, V., Prusiner, S. B., and Cohen F. E. (1997) *Curr. Opin. Struct. Biol. 7*, 53−59.
9. Uversky, V. N., Li, J., and Fink, A. L. (2001) *J. Biol. Chem. 276*, 10737−10744.
10. El-Agnaf, O. M., Jakes, R., Curran, M. D., and Wallace, A. (1998) *FEBS Lett. 440*, 67−70.
11. Narhi, L., Wood, S. J., Steavenson, S., Jiang, Y., Wu, G. M., Anafi, D., Kaufman, S. A., Martin, F., Denis, P., Louis, J. C., Wypych, J., Biere, A. L., and Citron, M. (1999) *J. Biol. Chem. 274*, 9843−9846.
12. Conway, K. A., Lee, S. J., Rochet, J. C., Ding, T. T., Williamson, R. E., and Lansbury, P. T., Jr. (2000) *Proc. Natl. Acad. Sci. U.S.A. 97*, 571−576.
13. Selkoe, D. J. (2001) *Physiol. Rev. 81*, 741−766.
14. Hu, H. Y. (2001) *Chin. Sci. Bull. 46*, 1−3.
15. Prusiner, S. B. (1996) *Trends Biochem. Sci. 21*, 482−487.
16. Uversky, V. N., and Fink, A. L. (2002) *FEBS Lett. 522*, 9−13.
17. Han, H., Weinreb, P. H., and Lansbury, P. T., Jr. (1995) *Chem. Biol*. *2*, 163−169.
18. El-Agnaf, O. M., Bodles, A. M., Guthrie, D. J. S., Harriott, P., and Irvine, G. B. (1998) *Eur. J. Biochem. 258*, 157−163.
19. Giasson, B. I., Murray, I. V. J., Trojanowski, J. Q., and Lee, V. M. Y. (2001) *J. Biol. Chem. 276*, 2380−2386.
20. Weinreb, P. H., Zhen, W., Poon, A. W., Conway, K. A., and Lansbury, P. T., Jr. (1996) *Biochemistry 35*, 13709−13715.
21. Hu, H. Y., Li, Q., Cheng, H. Q., and Du, H. N. (2001) *Biopolymers 62*, 15−21.
22. LeVine, H. (1999) *Methods Enzymol. 309*, 274−284.
23. Shearman, M. S. (1999) *Methods Enzymol. 309*, 716−723.
24. Clayton, D. E., and George, J. M. (1998) *Trends Neurosci. 21*, 249−254.
25. Bodles, A. M., Guthrie, D. J. S., Greer, B., and Irvine, G. B. (2001) *J. Neurochem. 78*, 384−395.
26. Serpell, L. C., Berriman, J., Jakes, R., Goedert, M., and Crowther, R. A. (2000) *Proc. Natl. Acad. Sci. U.S.A. 97*, 4897−4902.
27. Li, H. T., Du, H. N., Tang, L., Hu, J., and Hu, H. Y. (2002) *Biopolymers 64*, 221−226.
28. Shanmugam, V., Dion, P., Rochefort, D., Laganiere, J., Brais, B., and Rouleau, G. A. (2000) *Ann. Neurol. 48*, 798−802.
29. Kallberg, Y., Gustafsson, M., Persson, B., Thyberg, J., and Johansson, J. (2001) *J. Biol. Chem. 276*, 12945−12950.
30. Hinman, M. B., Jones, J. A., and Lewis, R. V. (2000) *Trends Biotechnol*. *18*, 374−379.
31. Lazaris, A., Arcidiacono, S., Huang, Y., Zhou, F. Y., Duguay, F., Chretien, N., Welsh, E. A., Soares, J. W., and Karatzas, C. N. (2002) *Science 295*, 472−476.
32. Kelly, J. W. (1996) *Curr. Opin. Struct. Biol. 6*, 11−17.
33. Harper, J. D., and Lansbury, P. T., Jr. (1997) *Annu. Rev. Biochem. 66*, 385−407.
34. Brown, D. R., Schmidt, B., and Kretzschmar, H. A. (1996) *Nature 380*, 345−347.
35. Gasset, M. A., Baldwin, M. A., Lloyd, D. H., Gabriel, J. M., Holtzman, D. M., Cohen, F., Fletterick, R., and Prusiner, S. B. (1992) *Proc. Natl. Acad. Sci. U.S.A. 89*, 10940−10944.
36. Lansbury, P. T., Jr., Costa, P. R., and Grifiths, J. M. (1995) *Nat. Struct. Biol. 2*, 990−998.
37. Terzi, E., Holzemann, G., and Seelig, J. (1995) *J. Mol. Biol*. *252*, 633−642.
38. King, C. Y., Tittanmann, P., Gross, H., Tittmann, P., Gross, H., Gebert, R., Aebi, M., and Wuthrich, K. (1997) *Proc. Natl. Acad. Sci. U.S.A. 94*, 6618−6622.
39. Baxa, U., Speransky, V., Steven, A. C., and Wickner, R. B. (2002) *Proc. Natl. Acad. Sci. U.S.A. 99*, 5253−5260.
40. Zahan, R., Liu, A., Luhrs, T., Riek, R., Schroetter, C., Garcia, F. L., Billeter, M., Calzolai, L., Wide, G., and Wuthrich, K. (2000) *Proc. Natl. Acad. Sci. U.S.A. 97*, 145−150.
41. Goldberg, M. S., and Lansbury, P. T., Jr. (2000) *Nat. Cell Biol. 2*, E115−E119.
42. Mezey, Z., Dehejia, A., Harta, G., Papp, M. I., Polymeropoulos, M. H., and Brownstein, M. J. (1998) *Nat. Med. 4*, 755−757.
43. Bucciantini, M., Giannoni, E., Chiti, F., Formigli, L., Zurdo, J., Taddei, N., Ramponi, G., Dobson, C. M., and Stefani, M. (2002) *Nature 416*, 507−511.
44. Tanaka, Y., Engelender, S., Rao, R. K., Igarashi, S., Wanner, T., Tanzi, R. E., Sawa, A. L., Dawson, V., Dawson, T. M., and Ross, C. A. (2001) *Hum. Mol. Genet. 10*, 919−926.

BI034028+